Anal. Chem. **2007,** *79,* 2525−2536

Atmospheric Pressure Covalent Adduct Chemical Ionization Tandem Mass Spectrometry for Double Bond Localization in Monoene- and Diene-Containing Triacylglycerols

Yichuan Xu† and J. Thomas Brenna*

Division of Nutritional Sciences, Cornell University, Ithaca, New York 14853

We report a method to elucidate the structure of triacylglycerols (TAGs) containing monoene or diene fatty acyl groups by atmospheric pressure covalent adduct chemical ionization (APCACI) tandem mass spectrometry using acetonitrile as an adduct formation reagent. TAGs were synthesized with the structures ABB and BAB, where A is palmitate (C16:0) and B is an isomeric C18 monoene unsaturated at position 9, 11, or 13 or an isomeric diene unsaturated at positions 9 and 11, 10 and 12, or 9 and 12. In addition to the species at *m/z* 54 observed in previous CI studies of fatty acid methyl esters, we also found that ions at *m/z* 42, 81, and 95 undergo covalent reaction with TAGs containing double bonds to yield ions at *m/z* 40, 54, 81, and 95 units greater than that of the parent TAG: $[M + 40]^+$, $[M + 54]^+$, $[M + 81]^+$, and $[M + 95]^+$ ions. When collisionally dissociated, these ions fragment to produce two or three diagnostic ions that locate the double bonds in the TAG. In addition, ions $[RCH{=}C{=}O + 40]^+$ and $[RCH{=}C{=}O + 54]^+$ formed from collisional dissociation are of strong abundance in MS/MS spectra, and collisional activation of these ions produces two intense confirmatory diagnostic ions in the MS^3 spectra. Fragment ions reflecting neutral loss of an *sn*-1-acyl group from $[M + 40]^+$ and $[M + 54]^+$ are more abundant than those reflecting neutral loss of an *sn*-2-acyl group, analogous to previous reports for protonated TAGs. The position of each acyl group on the glycerol backbone is thus determined by the relative abundances of these ions. Under the conditions in our instrument, the $[M + 40]^+$ adduct is at the highest signal and also yields all information about the double bond position and TAG stereochemistry. With the exception of geometries about the double bonds, racemic TAG isomers containing two monoenes or dienes and a saturate can be fully characterized by APCACI-MS/MS/MS.

Lipidomics is the emerging field of systems-level analysis and characterization of lipids and their interacting moieties. Mass spectrometry is a routine for lipid analysis; however, the complete structural elucidation of lipids remains an important analytical challenge.

Triacylglycerols (TAGs) are the most abundant dietary lipids. They constitute the major form of energy and essential fatty acid storage for plants and animals. TAGs are required at some minimal levels within cells to support specialized functions. Alterations in TAG synthesis and catabolism play important roles in obesity, atherosclerosis, insulin release from pancreatic β cells, and alcohol-induced hepatic dysfunction, among many other functions.[1−7]

Considering that TAGs are made up of combinations of 3 fatty acyl groups from any of 20−50 fatty acids present in cells, the number of distinct molecular TAG species from biological extracts may number in the thousands. TAGs have been extensively studied by mass spectrometry, employing various ionization techniques, including electron ionization (EI),[8,9] chemical ionization (CI),[10−12] atmospheric pressure chemical ionization (APCI),[13−19] desorption chemical ionization (DCI),[20−22] field desorption (FD),[23,24] thermospray (TSP),[25,26] fast atom bombardment (FAB),[27−29] elec-

* To whom correspondence should be addressed. E-mail: jtb4@cornell.edu. Phone: (607) 255-9182. Fax: (607) 255-1033.

† Present address: Barr Laboratories, Northvale, NJ.

(1) Dhalla, N. S.; Elimban, V.; Rupp, H. *Mol. Cell. Biochem.* **1992**, *116*, 3−9.
(2) Goldberg, I. J. *J. Lipid Res.* **1996**, *37*, 693−707.
(3) Koyama, K.; Chen, G. X.; Wang, M. Y.; Lee, Y.; Shimabukuro, M.; Newgard, C. B.; Unger, R. H. *Diabetes* **1997**, *46*, 1276−1280.
(4) Saudek, C. D.; Eder, H. A. *Am. J. Med.* **1979**, *66*, 843−852.
(5) Shimabukuro, M.; Ohneda, M.; Lee, Y.; Unger, R. H. *J. Clin. Invest.* **1997**, *100*, 290−295.
(6) Stanley, W. C.; Lopaschuk, G. D.; McCormack, J. G. *Cardiovasc. Res.* **1997**, *34*, 25−33.
(7) Unger, R. H. *Diabetes* **1995**, *44*, 863−870.
(8) Hites, R. A. *Anal. Chem.* **1970**, *42*, 1736−&.
(9) Kallio, H.; Laakso, P.; Huopalahti, R.; Linko, R. R.; Oksman, P. *Anal. Chem.* **1989**, *61*, 698−700.
(10) Demirbuker, M.; Blomberg, L. G.; Olsson, N. U.; Bergqvist, M.; Herslof, B. G.; Jacobs, F. A. *Lipids* **1992**, *27*, 436−441.
(11) Marai, L.; Myher, J. J.; Kuksis, A. *Can. J. Biochem. Cell Biol.* **1983**, *61*, 840−849.
(12) Cheung, M.; Young, A. B.; Harrison, A. G. *J. Am. Soc. Mass Spectrom.* **1994**, *5*, 553−557.
(13) Huang, A. S.; Robinson, L. R.; Gursky, L. G.; Profita, R.; Sabidong, C. G. *J. Agric. Food Chem.* **1994**, *42*, 468−473.
(14) Neff, W. E.; Byrdwell, W. C. *J. Liq. Chromatogr.* **1995**, *18*, 4165−4181.
(15) Mottram, H. R.; Evershed, R. P. *Tetrahedron Lett.* **1996**, *37*, 8593−8596.
(16) Byrdwell, W. C.; Emken, E. A.; Neff, W. E.; Adlof, R. O. *Lipids* **1996**, *31*, 919−935.
(17) Neff, W. E.; Byrdwell, W. C. *J. Chromatogr., A* **1998**, *818*, 169−186.
(18) Neff, W. E.; List, G. R.; Byrdwell, W. C. *J. Liq. Chromatogr. Relat. Technol.* **1999**, *22*, 1649−1662.
(19) Byrdwell, W. C.; Neff, W. E. *Rapid Commun. Mass Spectrom.* **2002**, *16*, 300−319.
(20) Laakso, P.; Kallio, H. *Lipids* **1996**, *31*, 33−42.

10.1021/ac062055a CCC: $37.00
Published on Web 02/06/2007

trospray ionization (ESI),[30−35] and matrix-assisted laser desorption/ionization (MALDI).[36−38] These techniques typically yield information about the molecular weight, fatty acid carbon number, degree of unsaturation, and regiospecificity, but do not reveal the arrangement of double bonds, which is the single most significant structural property determining biological activity. A rapid, instrumental method for analysis of the double bond position in TAGs is required.

Conventional approaches for determination of the double bond position by mass spectrometry rely on an initial hydrolysis of fatty acyl groups, followed by chemical derivatization to enhance the yield of diagnostically useful fragment ions obtained upon collisional dissociation. Single acyl groups are esterified with charge-localizing groups such as 4,4-dimethyloxalone (DMOX) or picolinyl esters with subsequent analysis of charge-remote fragmentation. The disadvantages of these methods have been discussed[39] and include the need for derivatization chemistry prior to analysis and generally low sensitivity.

In previous work,[39−42] we have demonstrated a rapid technique for double bond localization in fatty acid methyl esters (FAMEs) based on chemical derivatization of neutral FAMEs in the gas phase, which we recently termed "covalent adduct chemical ionization" (CACI).[43] The CI mass spectrum of CH_3CN in a 3D internal ionization ion trap includes ions at m/z 40 and 42, formed by loss or gain of H, and an ion at m/z 54.[44,45] It has been demonstrated that an ion/molecule reaction between $[C_2H_2N]^+$ (m/z 40) and neutral CH_3CN results in the formation of an intermediate $[C_4H_5N_2]^+$ at m/z 81, which loses HCN to form the (1-methyleneimino)-1-ethenylium (MIE, $CH_2{=}C{=}N^+{=}CH_2$) ion at m/z 54.[46] MIE in turn reacts with carbon−carbon double bonds in FAMEs to form a covalent adduct ion appearing at 54 mass units greater than that of the parent FAME, $[M + 54]^+$. Isolation and collisional activation of the $[M + 54]^+$ ions yields fragments corresponding to bond cleavage at specific locations in FAMEs. The two ions that are normally of greatest abundance contain either the α- or ω-carbon atoms and have masses unique to the positions of double bonds within the FAME. Early studies of this reaction included double bond identification in monoene hydrocarbons and polyene alcohols,[47,48] as well as monoene FAMEs.[49]

TAGs are neutral molecules that can be analyzed by high-temperature gas chromatography (GC) but for lipidomics applications are more commonly analyzed from a liquid by ESI. ESI is a soft ionization technique which excels at analysis of charged or high proton affinity compounds. To adapt CACI to the liquid phase, we investigated the use of APCI as a source for reagent ions for covalent adduct formation with TAGs, similar to our gas-phase FAME analysis. Conditions were first developed to produce adequate levels of reagent ions for derivatization of neutral TAGs, under conditions we refer to as atmospheric pressure covalent adduct chemical ionization (APCACI). TAGs of the forms ABB and BAB (*sn*-1,2,3) were synthesized, where B is a monoene or diene fatty acyl group of one of several isomers and A is palmitic acid (hexadecanoic acid, 16:0). The resulting ions were characterized for their ability to form diagnostically useful fragments by single-, double-, and triple-stage mass spectrometry.

EXPERIMENTAL SECTION

Chemicals. The following fatty acids were purchased from Matreya, Inc. (Pleasant Gap, PA): 9*c*-octadecenoic acid (oleic acid), 9*c*,12*c*-octadecadienoic acid, 9*c*,11*t*-octadecadienoic acid (rumenic acid), and 10*t*,12*c*-octadecadienoic acid. 11*c*-Octadecenoic acid (vaccenic acid), 13*c*-octadecenoic acid, 1,3-dicyclohexylcarbodiimide, and 4-(dimethylamino)pyridine were purchased from Sigma Chemical Co. (St. Louis, MO). 1-Palmitin and 2-palmitin were obtained from Research Plus, Inc. (Manasquan, NJ). Thin layer chromatography (TLC) plates were obtained from Analtech Inc. (Newark, DE). The following TAGs were synthesized by esterification of fatty acids with *sn*-1- or *sn*-2-monopalmitoylglycerol as reported elsewhere:[50] *rac*-glyceryl-1,3-9*c*-octadecenoate-2-palmitate [(9-18:1/16:0/9-18:1)-TAG], *rac*-glyceryl-1-palmitate-2,3-9*c*-octadecenoate [(16:0/9-18:1/9-18:1)-TAG], *rac*-glyceryl-1,3-11*c*-octadecenoate-2-palmitate [(11-18:1/16:0/11-18:1)-TAG], *rac*-glyceryl-1-palmitate-2,3-11*c*-octadecenoate [(11-18:1/16:0/11-18:1)-TAG], *rac*-glyceryl-1,3-13*c*-octadecenoate-2-palmitate [(13-18:1/16:0/13-18:1)-TAG], *rac*-glyceryl-1-palmitate-2,3-13*c*-octadecenoate [(16:0/13-18:1/13-18:1)-TAG], *rac*-glyceryl-1,3-9*c*,11*t*-octadecadienoate-2-palmitate [(9,11-18:2/16:0/9,11-18:2)-TAG], *rac*-glyceryl-1-palmitate-2,3-9*c*,11*t*-octadecadienoate [(9,11-18:2/16:0/9,11-18:2)-TAG], *rac*-glyceryl-1,3-10*t*,12*c*-octadecadienoate-2-palmitate [(10,12-18:2/16:0/10,12-18:2)-TAG], *rac*-glyceryl-1-palmitate-2,3-10*t*,12*c*-octadeca-

(21) Stroobant, V.; Rozenberg, R.; Bouabsa, E. M.; Deffense, E.; Dehoffmann, E. *J. Am. Soc. Mass Spectrom.* **1995**, *6*, 498−506.
(22) Anderson, M. A.; Collier, L.; Dilliplane, R.; Ayorinde, F. O. *J. Am. Oil Chem. Soc.* **1993**, *70*, 905−908.
(23) Lehmann, W. D.; Kessler, M. *Biomed. Mass Spectrom.* **1983**, *10*, 220−226.
(24) Evans, N.; Games, D. E.; Harwood, J. L.; Jackson, A. H. *Biochem. Soc. Trans.* **1974**, *2*, 1091−1093.
(25) Sundin, P.; Larsson, P.; Wesen, C.; Odham, G. *Biol. Mass Spectrom.* **1992**, *21*, 633−641.
(26) Kim, H. Y.; Salem, N. *Anal. Chem.* **1987**, *59*, 722−726.
(27) Lamberto, M.; Saitta, M. *J. Am. Oil Chem. Soc.* **1995**, *72*, 867−871.
(28) Hori, M.; Sahashi, Y.; Koike, S.; Yamaoka, R.; Sato, M. *Anal. Sci.* **1994**, *10*, 719−724.
(29) Evans, C.; Traldi, P.; Bambagiottialberti, M.; Giannellini, V.; Coran, S. A.; Vincieri, F. F. *Biol. Mass Spectrom.* **1991**, *20*, 351−356.
(30) Duffin, K. L.; Henion, J. D.; Shieh, J. J. *Anal. Chem.* **1991**, *63*, 1781−1788.
(31) Cheng, C. F.; Gross, M. L. *Anal. Chem.* **1998**, *70*, 4417−4426.
(32) Hsu, F. F.; Turk, J. *J. Am. Soc. Mass Spectrom.* **1999**, *10*, 587−599.
(33) Hvattum, E. *Rapid Commun. Mass Spectrom.* **2001**, *15*, 187−190.
(34) Fard, A. M.; Turner, A. G.; Willett, G. D. *Aust. J. Chem.* **2003**, *56*, 499−508.
(35) Segall, S. D.; Artz, W. E.; Raslan, D. S.; Ferraz, V. P.; Takahashi, J. A. *Food Res. Int.* **2005**, *38*, 167−174.
(36) Asbury, G. R.; Al-Saad, K.; Siems, W. F.; Hannan, R. M.; Hill, H. H. *J. Am. Soc. Mass Spectrom.* **1999**, *10*, 983−991.
(37) Robins, C.; Limbach, P. A. *Rapid Commun. Mass Spectrom.* **2003**, *17*, 2839−2845.
(38) Calvano, C. D.; Palmisano, F.; Zambonin, C. G. *Rapid Commun. Mass Spectrom.* **2005**, *19*, 1315−1320.
(39) Michaud, A. L.; Diau, G. Y.; Abril, R.; Brenna, J. T. *Anal. Biochem.* **2002**, *307*, 348−360.
(40) Van Pelt, C. K.; Brenna, J. T. *Anal. Chem.* **1999**, *71*, 1981−1989.
(41) Van Pelt, C. K.; Carpenter, B. K.; Brenna, J. T. *J. Am. Soc. Mass Spectrom.* **1999**, *10*, 1253−1262.
(42) Michaud, A. L.; Yurawecz, M. P.; Delmonte, P.; Corl, B. A.; Bauman, D. E.; Brenna, J. T. *Anal. Chem.* **2003**, *75*, 4925−4930.
(43) Lawrence, P.; Brenna, J. T. *Anal. Chem.* **2006**, *78*, 1312−1317.
(44) Moneti, G.; Pieraccini, G.; Dani, F. R.; Catinella, S.; Traldi, P. *Rapid Commun. Mass Spectrom.* **1996**, *10*, 167−170.
(45) Moneti, G.; Pieraccini, G.; Favretto, D.; Traldi, P. *J. Mass Spectrom.* **1998**, *33*, 1148−1149.
(46) Oldham, N. J. *Rapid Commun. Mass Spectrom.* **1999**, *13*, 1694−1698.
(47) Moneti, G.; Pieraccini, G.; Dani, F. R.; Turillazzi, S.; Favretto, D.; Traldi, P. *J. Mass Spectrom.* **1997**, *32*, 1371−1373.
(48) Moneti, G.; Pieraccini, G.; Favretto, D.; Traldi, P. *J. Mass Spectrom.* **1999**, *34*, 1354−1360.
(49) Oldham, N. J. S. A. *Rapid Commun. Mass Spectrom.* **1999**, *13*, 331−336.
(50) Jie, M.; Lam, C. C.; Yan, B. F. Y. *J. Chem. Res., Synop.* **1993**, 141−141.

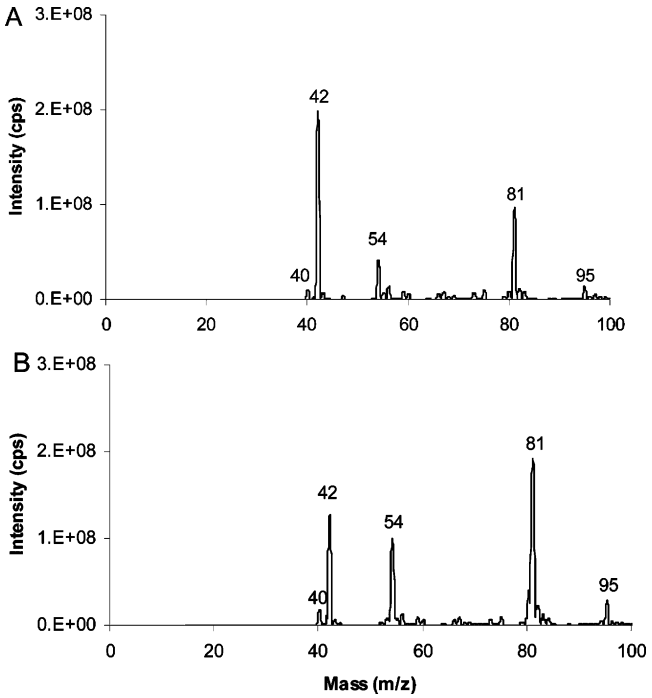

Figure 1. APCI mass spectra of CH_3CN. (A) N_2 and (B) He were used as the nebulizer and auxiliary gases. The spectra include ions at *m/z* 40 and 42, formed by loss and gain of H, and at *m/z* 54, 81, and 95, generated by ion/molecule reactions of acetonitrile.

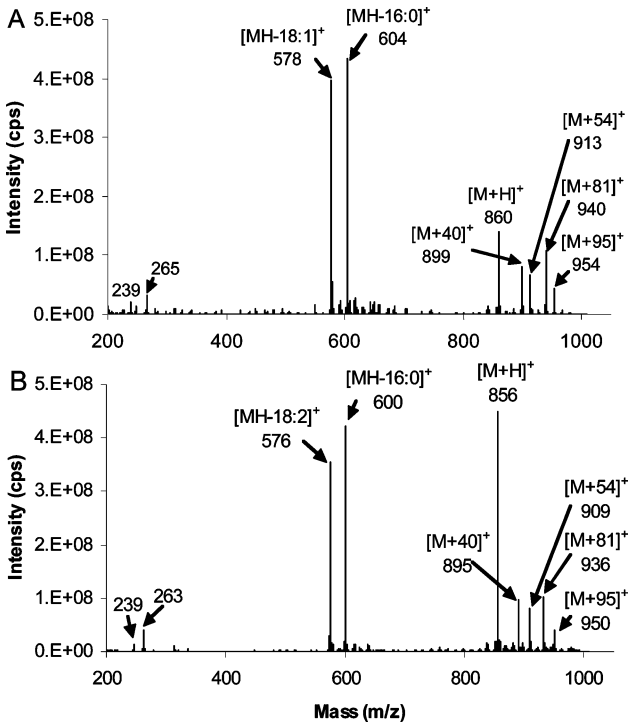

Figure 2. APCACI-MS spectra of (A) (16:0/9-18:1/9-18:1)-TAG and (B) (16:0/9,12-18:2/9,12-18:2)-TAG: MH^+, $[M - RCO_2]^+$ ions arising from loss of fatty acid moieties, $[M + 54]^+$, $[M + 40]^+$, $[M + 81]^+$, and $[M + 95]^+$.

dienoate [(10,12-18:2/16:0/10,12-18:2)-TAG], *rac*-glyceryl-1,3-9*c*,-12*c*-octadecadienoate-2-palmitate [(9,12-18:2/16:0/9,12-18:2)-TAG], *rac*-glyceryl-1-palmitate-2,3-9*c*,12*c*-octadecadienoate [(9,12-18:2/16:0/9,12-18:2)-TAG]. Solvents were obtained from Aldrich Chemical Co. (Milwaukee, WI).

Instrumentation. An ABI MDS/Sciex QTRAP 2000 triple-quadrupole linear ion trap mass spectrometer was employed in the APCI positive ion mode. The data acquisition and processing software was Analyst 1.4, and MS-1 masses were centroided to reduce clutter in the spectrum. Helium, rather than the conventional N_2, was used as the nebulizer, auxiliary, and collision gas. The heated pneumatic nebulizer probe conditions were 350 °C, 65 psi nebulizing gas pressure, 25 psi auxiliary gas pressure, and 50 psi curtain gas pressure. The needle current was set at 2.0 μA. The declustering potential was set at 90 V. Samples were delivered into the ionization source with a syringe pump by infusion at a flow rate of 25 μL/min of the TAG dissolved in chloroform/acetonitrile (1/9) to a final concentration of 100 μg/mL. Data were acquired for 1 min per spectrum. Under these conditions, a continuous plasma discharge is observed in the region from the quartz tube to the curtain plate. Chemically active adducts were not detected under conventional APCI conditions; the plasma glow was essential. This may have been due to the large ionization volume within which the neutral TAG and active ions interacted within the plasma; further experiments are required to clarify this point. After approximately 300 h of analysis, we found that the heater coil, though still functional, had cracked at a stress point apparently due to metal degradation by the plasma and high temperature.

TAG molecular species were directly ionized in the positive ion mode by APCACI. Tandem mass spectrometry of TAGs was performed by collisional activation with He gas. MS/MS/MS was performed with the third quadrupole operated in linear ion trap mode. The degree of collisional activation was adjusted through variation of the collision energy.

RESULTS AND DISCUSSION

APCI-MS of Acetonitrile. Figure 1 presents APCI mass spectra of acetonitrile using (A) N_2 and (B) He as the nebulizer and auxiliary gases, respectively. They consist of five main ionic species at *m/z* 40 $[M - H]^+$, 42 $[M + H]^+$, 54, 81, and 95. The former three ions are in agreement with previous investigations of acetonitrile CI.[43−45] It was demonstrated that an ion/molecule reaction between $[C_2H_2N]^+$ (*m/z* 40) and neutral acetonitrile results in the formation of a $[C_4H_5N_2]^+$ (*m/z* 81) intermediate, which loses HCN to yield the $[C_3H_4N]^+$ *m/z* 54 ion, identified as MIE. *m/z* 95 is likely to correspond to $C_5H_7N_2^+$ originating from reaction of *m/z* 54 ions with neutral acetonitrile (*m/z* 41). The *m/z* 54 ions are formed at about 20% and 70% abundances of the $[C_2H_2N]^+$ ions when using N_2 and He, respectively. In this work, He was used as the nebulizer and auxiliary gas.

APCACI-MS of TAGs. Parts A and B of Figure 2 show the single-stage MS of a TAG of the form ABB with a monoene or diene as fatty acyl group B, 16:0/9-18:1/9-18:1 and 16:0/9,12-18:2/9,12-18:2. The major ions are MH^+, $[M - RCO_2]^+$ ions from loss of fatty acid moieties, $[M + 54]^+$, $[M + 40]^+$, $[M + 81]^+$, and $[M + 95]^+$. $[RCO]^+$ (ketene ions) derived from the fatty acyl moieties themselves were also present at low relative abundance. The MH^+ ion intensity for the diene-containing TAG is about double the intensity of the monoene-containing TAG compared to the acyl and ketene neutral loss peaks, relative to the base peak. The $[M + 40]^+$ species indicates that the $[C_2H_2N]^+$ ion from acetonitrile adds to the TAG, and analogous ions have been

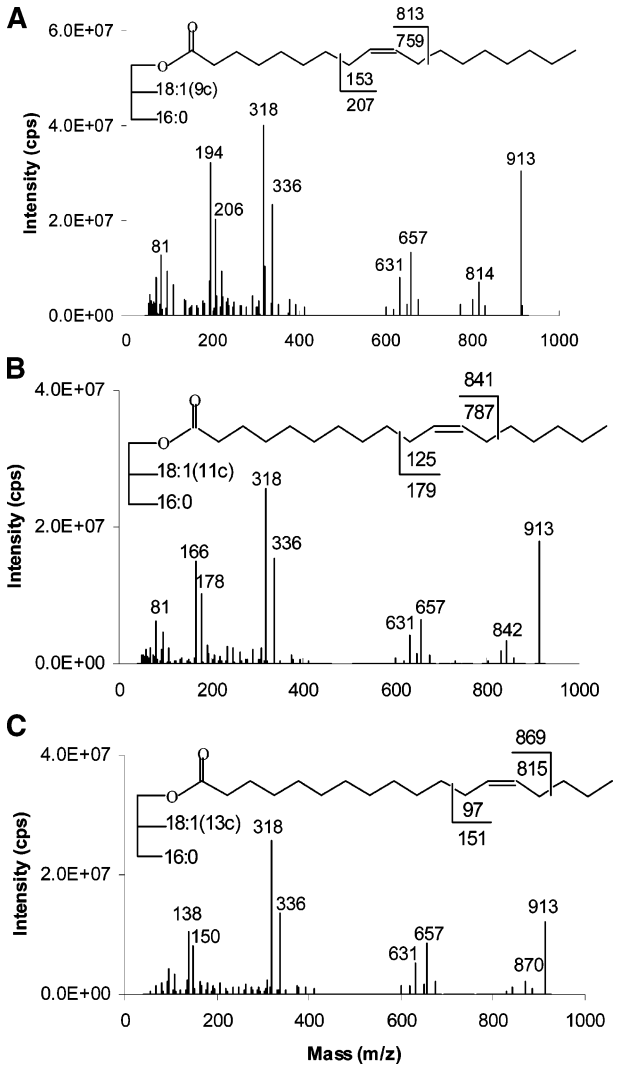

Figure 3. $[M + 54]^+$-based APCACI-MS/MS spectra of (A) (16:0/9-18:1/9-18:1)-TAG, (B) (16:0/11-18:1/11-18:1)-TAG, and (C) (16:0/13-18:1/13-18:1)-TAG. Collisional dissociation of *m/z* 913 yields diagnostic ions corresponding to cleavage either vinylic or allylic to the site of the erstwhile double bond.

reported in the acetonitrile CI mass spectra of monoene FAMEs.[49] The $[M + 54]^+$ ion corresponds to the addition of $[C_3H_4N]^+$ to the TAG, consistent with results obtained for FAMEs in our previous papers.[43−47]

We first focus interest on the $[M + 54]^+$ species since it is by far the best studied adduct ion for analysis of the position of double bonds in the carbon chain. The mass spectra are typified by that of *rac*-glyceryl-1,3-9-octadecenoate-2-palmitate, in which specific ions are observed: MH^+ at *m/z* 860, two $[M - RCO_2]^+$ ions at *m/z* 604 and 578, corresponding to loss of palmitate to yield $[BB]^+$ and loss of octadecenoate to give $[AB]^+$, respectively, $[M + 54]^+$ at *m/z* 913, $[M + 40]^+$ at *m/z* 899, and $[M + 81]^+$ at *m/z* 940. Starting with $[M + 54]^+$, we discuss spectra arising from collisional dissociation of all the adduct ions.

$[M + 54]^+$. *APCACI-MS/MS of Monoene-Containing TAGs.* Figure 3 presents the APCACI-MS/MS spectra of a series of three ABB TAGs isomeric only in the position of the double bond on the monoene group: (16:0/9-18:1/9-18:1)-TAG, (16:0/11-18:1/11-18:1)-TAG, and (16:0/13-18:1/13-18:1)-TAG. Mass spectra are generated by collisional dissociation of the isolated $[M + 54]^+$ ions. All of the MS/MS spectra show abundant $[RCO_2H + 54]^+$ at *m/z* 336, the adduct of monoene fatty acyl moieties and MIE. MS/MS fragmentation of $[M + 54]^+$ of TAGs also resulted in the adducts of ketene (generated from fatty acyl groups) and *m/z* 54 ions $[RCH{=}C{=}O + 54]^+$, analogous to the $[M + 54 - 32]^+$ loss of methanol in the corresponding FAMEs reported previously. The $[RCH{=}C{=}O + 54]^+$ peak at *m/z* 318 is the base peak. The spectra also contain ions $[BB + 54]^+$ and $[AB + 54]^+$ at *m/z* 657 and 631, reflecting neutral loss of 16:0 and 18:1, respectively, from $[M + 54]^+$.

Upon collisional activation, $[M + 54]^+$ undergoes fragmentation to yield diagnostic ions. These ions correspond to cleavage either vinylic or allylic to the site of the erstwhile double bond, as indicated in the structures in Figure 3. The site of bond breakage for diagnostically important ions and the ion mass expected for homolytic bond breakage, with and without the *m/z* 54 adduct, are displayed in the structure of the TAG in each spectrum. Consistent with our nomenclature for CACI of FAMEs, we define the α diagnostic ion as containing the remaining glycerol lipid and the ω diagnostic ion as containing the terminal methyl group of the fatty acyl chain. The strongest α diagnostic ion is due to allylic cleavage and appears 1 unit above the expected mass due to H transfer from a neutral group to an ion. In contrast, the strong ω diagnostic ions are observed vinylic and allylic to the former site of the double bond and are 1 unit *lower* than those expected from homolytic cleavage. Smaller satellite ions at ±14 units were also observed. The ω diagnostic ions for (16:0/9-18:1/9-18:1)-TAG, (16:0/11-18:1/11-18:1)-TAG, and (16:0/13-18:1/13-18:1)-TAG appear at *m/z* 194−206, 166−178, and 138−150, respectively, while the α diagnostic ions for these TAGs appear at *m/z* 814, 842, and 870, respectively. These spectra show that TAGs containing isomeric monoenes can be differentiated on the basis of APCACI collisional dissociation.

Abundant fragment ions in the *m/z* range from 50 to 110 were also observed in the spectra in Figure 3. These include a series of alkyl ions at *m/z* 57, 71, etc. and an unsaturated series at *m/z* 67, 81, 95, etc. Similar ion series were observed under ESI condtions.[32]

APCACI-MS^3 of Monoene-Containing TAGs. An important feature of unsaturated TAG fragmentation is the abundant $[RCH{=}C{=}O + 54]^+$, the ketene adduct ion. The mass of these ions suggests that they should undergo a similar charge-driven rearrangement and fragmentation as $[M + 54]^+$ of FAMEs to yield α and ω diagnostic ions. This hypothesis is supported by MS^3 experiments performed on abundant $[RCH{=}C{=}O + 54]^+$ ion at *m/z* 318. The resultant APCACI-MS/MS/MS spectra are displayed in Figure 4. By analogy to the fragmentation of FAME $[M + 54]^+$, each isomer yields fragments characteristic of the double bond position and corresponding to allylic cleavage. The α diagnostic ions of the *m/z* 318 ion, $[RCH{=}C{=}O + 54]^+$, where fatty acyl groups are 9-18:1, 11-18:1, and 13-18:1, appear at *m/z* 220, 248, and 276, respectively, at mass 1 unit higher than would be expected from homolytic bond cleavage. The ω diagnostic ions of corresponding *m/z* 318 ions appear at *m/z* 206, 178, and 150, 1 mass unit lower than expected from homolytic cleavage. Thus, each of the three positional isomers yields a strong and unique APCACI-MS^3 spectrum that permits unambiguous identification of the double bond location.

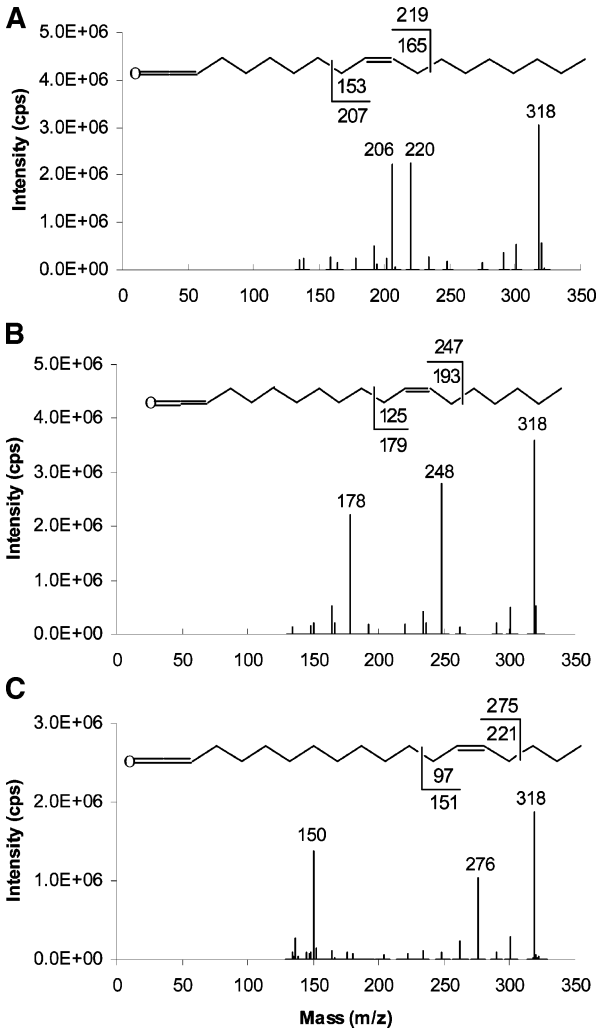

Figure 4. [M + 54]$^+$-based APCACI-MS/MS spectra of (A) (16:0/9-18:1/9-18:1)-TAG, (B) (16:0/11-18:1/11-18:1)-TAG, and (C) (16:0/13-18:1/13-18:1)-TAG. The [ketene + 54]$^+$ ions at *m/z* 318 derived from MS/MS of [M + 54] of monoene TAGs were selected and collisionally dissociated (*m/z* 913 → *m/z* 318 → products) to yield a pair of diagnostic ions. Each of these pairs of diagnostic ions is unique to a particular isomer.

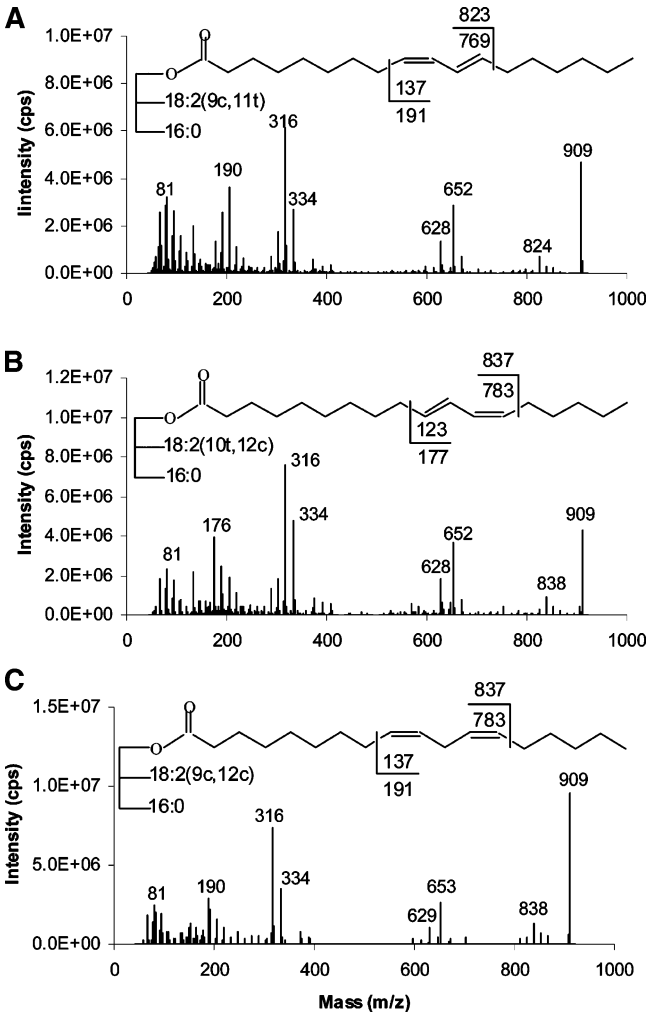

Figure 5. [M + 54]$^+$-based APCACI-MS/MS spectra of *m/z* 909 from (A) (16:0/9,11-18:2/9,11-18:2)-TAG, (B) (16:0/10,12-18:2/10,-12-18:2)-TAG, and (C) (16:0/9,12-18:2/9,12-18:2)-TAG. Cleavages directly before the first double bond and immediately after the second, as shown in the structures, give rise to diagnostic ions.

APCACI-MS/MS of Diene-Containing TAGs. In Figure 5 we present the APCACI-MS/MS spectra of TAGs containing 18:2 fatty acyl groups, two with conjugated double bonds, and the acyl group of linoleic acid, with a homoallylic (methylene-interrupted) set of double bonds. The spectra show abundant [M + 54]$^+$ at *m/z* 909, [RCO_2H + 54]$^+$ at *m/z* 334, [ketene + 54]$^+$ at *m/z* 316, [BB]$^+$ at *m/z* 652 or 653, and [AB]$^+$ at *m/z* 628 or 629 as well as two diagnostic ions.

For TAGs containing conjugated double bonds, C−C cleavage occurs vinylic to the erstwhile double bond, producing α and ω diagnostic ions. Parts A and B of Figure 5 show MS/MS spectra of TAGs containing two conjugated 18:2 bonds, the 9,11 and 10,-12 isomers, respectively. The α and ω diagnostic ions for (16:0/9,11-18:2/9,11-18:2)-TAG appear at *m/z* 824 and 190, respectively, while the analogous ions for (16:0/10,12-18:2/10,11-18:2)-TAG occur at *m/z* 838 and 176, respectively. As with the TAG containing the monoenes, the α ions appear 1 unit above the expected mass while the ω ions appear at masses 1 unit lower than those expected from homolytic cleavage.

For TAGs containing homoallylic dienes, collisional dissociation of the [M + 54]$^+$ ion also proceeds via bond cleavage at a position vinylic to the site of the original double bond. For (9,12-18:2/16:0/9,12-18:2)-TAG, cleavage directly before the first double bond and immediately after the second gives rise to the diagnostic ions at *m/z* 190 and 838, as indicated in Figure 5C. As with the TAG containing monoenes, the α ions appear 1 unit above the expected mass while the ω ions appear at masses 1 unit lower than those expected from homolytic cleavage.

APCACI-MS^3 of Diene-Containing TAGs. Figure 6 shows the APCACI-MS/MS/MS spectra of a series of TAGs containing dienes. The [ketene + 54]$^+$ ions at *m/z* 316 derived from MS/MS of [M + 54]$^+$ of the TAG were selected and collisionally dissociated to yield MS^3 spectra. In Figure 6A,B, ketene derived from a TAG containing a 9,11-18:2 conjugated fatty acyl group yields *m/z* 190 and 232 diagnostic ions and can readily be distinguished from ketene derived from a TAG containing a 10,-12-18:2 conjugated fatty acyl group, where *m/z* 176 and 246 are the diagnostic ions. The APCACI-MS/MS/MS spectrum of ketene derived from (16:0/9,12-18:2/9,12-18:2)-TAG is shown in Figure 6C. The diagnostic ions are *m/z* 190 and 246. These ions originate

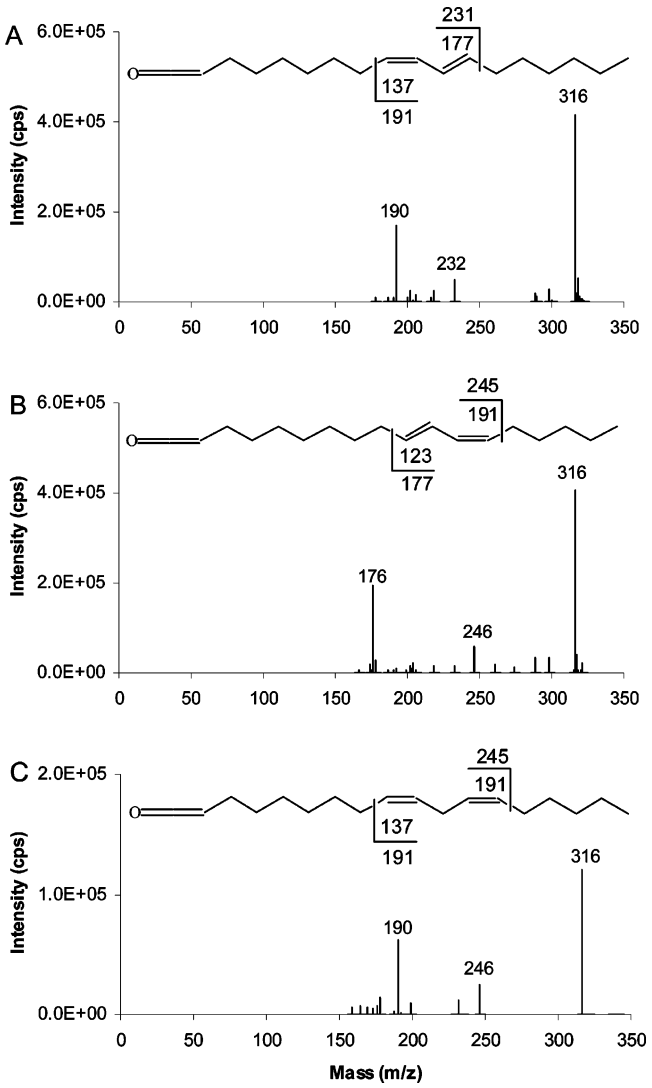

Figure 6. $[M + 54]^+$-based APCACI-MS/MS/MS spectra of (A) (16:0/9,11-18:2/9,11-18:2)-TAG, (B) (16:0/10,12-18:2/10,12-18:2)-TAG, and (C) (16:0/9,12-18:2/9,12-18:2)-TAG. The [ketene + 54]$^+$ ions derived from $[M + 54]^+$ of diene TAGs (*m/z* 909 → 318 → products) yield two fragments characteristic of the double bond position.

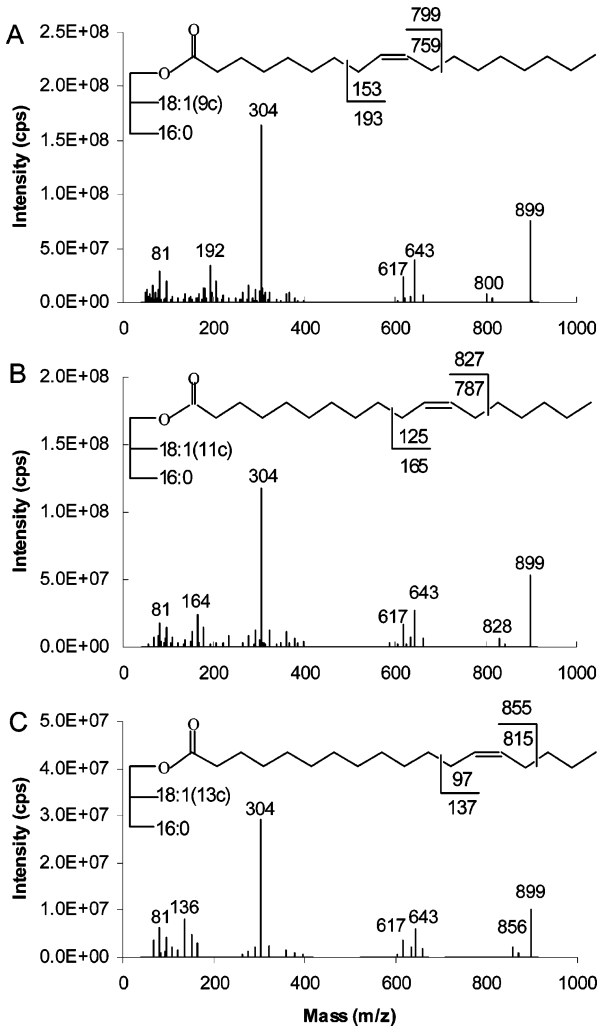

Figure 7. $[M + 40]^+$-based APCACI-MS/MS spectra of *m/z* 899 for (A) (16:0/9-18:1/9-18:1)-TAG, (B) (16:0/11-18:1/11-18:1)-TAG, and (C) (16:0/13-18:1/13-18:1)-TAG. Specific cleavages at the allylic carbons shown in the structures at the top of each spectrum give rise to a pair of diagnostic ions.

from C−C bond cleavage at a position that is vinylic to the site of the former double bonds, and as with the TAG containing monoenes, the α ions appear 1 unit above the expected mass while ω ions appear at masses 1 unit lower than those expected from homolytic cleavage. These spectra show fragments analogous to those presented in Figure 4.

$[M + 40]^+$. *APCACI-MS/MS of Monoene-Containing TAGs.* The APCACI-MS/MS spectra of $[M + 40]^+$ adducts of (16:0/9-18:1/9-18:1)-TAG, (16:0/11-18:1/11-18:1)-TAG, and (16:0/13-18:1/13-18:1)-TAG are shown in Figure 7. The base peaks obtained for all three TAGs are ions at *m/z* 304 arising from the adducts of ketene and *m/z* 40 ions $[RCH{=}C{=}O + 40]^+$. Unlike the $[M + 54]^+$ MS/MS spectra of Figure 3, no loss of an acyl group is observed from the $[M + 40]^+$ ion. The other expected products for all TAGs are *m/z* 643 and 617 arising by neutral loss of 16:0 and 18:1, respectively, from the $[M + 40]^+$ complex. Abundant fragment ions in the *m/z* range from 50 to 110 were also observed in the spectra in Figure 7. These include a series of alkyl ions at *m/z* 57, 71, etc. and an unsaturated series at *m/z* 67, 81, and 95, similar to those observed under ESI condtions.[32]

The spectra contain two diagnostic ions, with dominant cleavage allylic to the former site of the double bond, as indicated in the structures in Figure 7. Again, the α ions appear 1 unit above the expected mass, thus implying hydrogen transfer from the neutral group to the ion, while ω ions appear at masses 1 unit lower than those expected from homolytic cleavage, indicating the reverse. For (16:0/9-18:1/9-18:1)-TAG, the ion appearing at *m/z* 800 is the α diagnostic ion and that at *m/z* 192 is the ω diagnostic ion. The analogous ions are found at *m/z* 828 and 164 for (16:0/11-18:1/11-18:1)-TAG and at *m/z* at 856 and 136 for (16:0/13-18:1/13-18:1)-TAG, respectively. Satellite ions at ±14 units are also observed at lower intensity.

APCACI-MS^3 of Monoene-Containing TAGs. The results presented above show that $[RCH{=}C{=}O + 40]^+$ ions at *m/z* 304, the adduct of ketene from the fatty group and $C_2H_2N^+$, are generated in MS/MS. The generation of $[RCH{=}C{=}O + 40]^+$ creates the opportunity to analyze the product ions in MS^3 to confirm the double bond location in unsaturated fatty acyl substituents, indicated in the MS/MS data. Diagnostic ions produced from

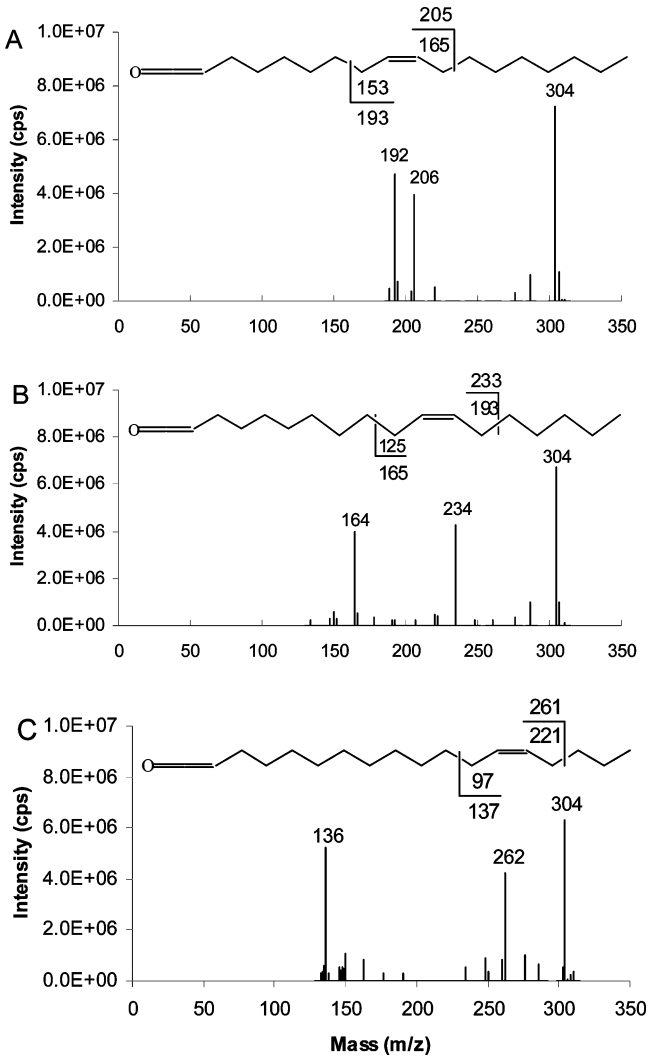

Figure 8. $[M + 40]^+$-based APCACI-MS/MS spectra of *m/z* 899 → *m/z* 304 → products for (A) (16:0/9-18:1/9-18:1)-TAG, (B) (16:0/11-18:1/11-18:1)-TAG, and (C) (16:0/13-18:1/13-18:1)-TAG. The $[\text{ketene} + 40]^+$ ions at *m/z* 304 derived from MS/MS of $[M + 40]^+$ of monoene TAGs were selected and collisionally dissociated to yield a pair of diagnostic ions. Each of these pairs of diagnostic ions is unique to a particular isomer.

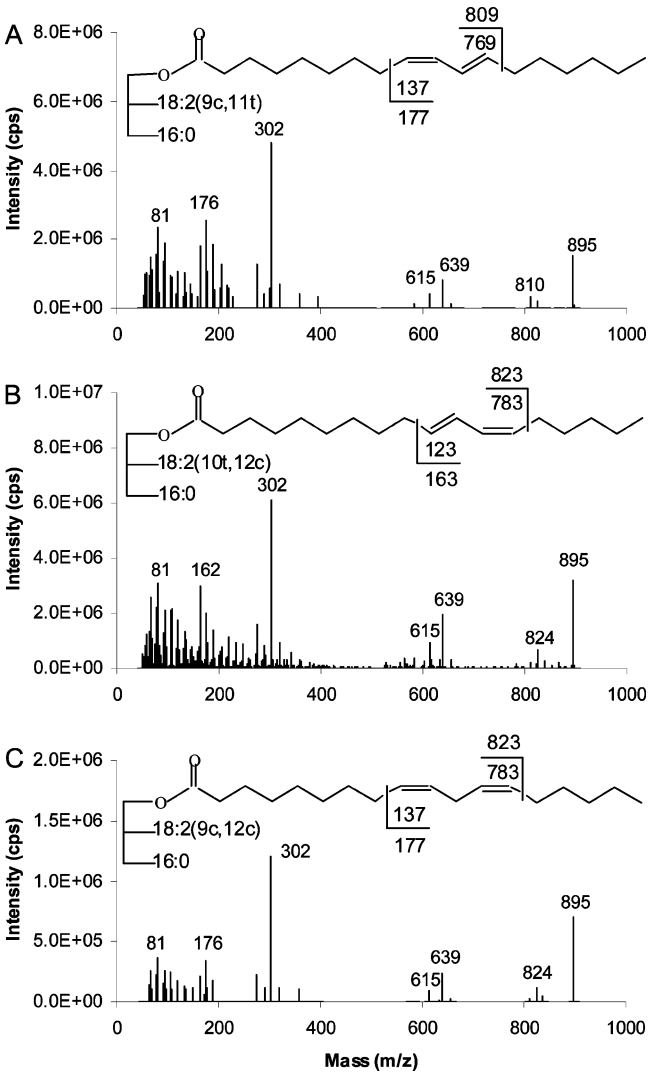

Figure 9. $[M + 40]^+$-based APCACI-MS/MS spectra for *m/z* 895 of (A) (16:0/9,11-18:2/9,11-18:2)-TAG, (B) (16:0/10,12-18:2/10,12-18:2)-TAG, and (C) (16:0/9,12-18:2/9,12-18:2)-TAG. Cleavages directly before the first double bond and immediately after the second, as shown in the structures, give rise to diagnostic ions.

collisional dissociation of these ions correspond to C−C bond cleavage adjacent to either allylic site of the double bond and produce the α diagnostic ion containing the ketene group and the ω diagnostic ion containing the terminal methyl group. Diagnostic ions analogous to those observed in Figure 4 for the $[\text{RCH=C=O} + 54]^+$ ions are observed. The α diagnostic ion appears at mass 1 unit higher than would be expected from homolytic bond cleavage, while the ω diagnostic ion appears at 1 mass unit lower than expected from homolytic cleavage. Figure 8 shows MS/MS/MS spectra of (16:0/9-18:1/9*c*-18:1)-TAG, (16:0/11-18:1/11-18:1)-TAG, and (16:0/13-18:1/13-18:1)-TAG. The α diagnostic ions resulting from the $[\text{RCH=C=O} + 40]^+$ ion at *m/z* 304, where fatty acyl groups are 9-18:1, 11-18:1, and 13-18:1, appear at *m/z* 206, 234, and 262, respectively. The ω diagnostic ions of the corresponding ions at *m/z* 304 appear at *m/z* 192, 164, and 136. MS^3 of $[\text{RCH=C=O} + 40]^+$ is dominated by diagnostic ion fragments that stand out more clearly than diagnostic ions in MS/MS (Figure 7) to unequivocally confirm the double bond location.

APCACI-MS/MS of Diene-Containing TAGs. Figure 9 shows the APCACI-MS/MS spectra of TAGs containing 18:2 fatty acyl groups derived from collisional activation of $[M + 40]^+$ ions. The common products observed for all TAGs are $[M + 40]^+$ at *m/z* 895, $[\text{RCH=C=O} + 40]^+$ at *m/z* 302, and $[BB]^+$ at *m/z* 639 and $[AB]^+$ at *m/z* 615 arising, respectively, by loss of C16:0 and C18:2 from the $[M + 40]^+$ ions.

Spectra for TAGs containing 9,11-CLA and 10,12-18:2 isomers are presented in parts A and B, respectively, of Figure 9. The α and ω diagnostic ions, at masses predicted by cleavage vinylic to the double bond, are observed at *m/z* 810 and 176 for (16:0/9,-11-18:2/9,11-18:2)-TAG and *m/z* 824 and 162 for (16:0/10,12-18:2/10,11-18:2)-TAG. For (9,12-18:2/16:0/9,12-18:2)-TAG, vinylic cleavage is also observed to give rise to the diagnostic ions at *m/z* 176 and 824, as indicated in Figure 9C. As with the TAG containing monoenes, the α ions appear 1 unit above the expected mass while the ω ions appear at masses 1 unit lower than those expected from homolytic cleavage.

$APCACI\text{-}MS^3$ of Diene-Containing TAGs. As with TAGs containing monoene groups, collisional activation of the $[\text{ketene} + 40]^+$

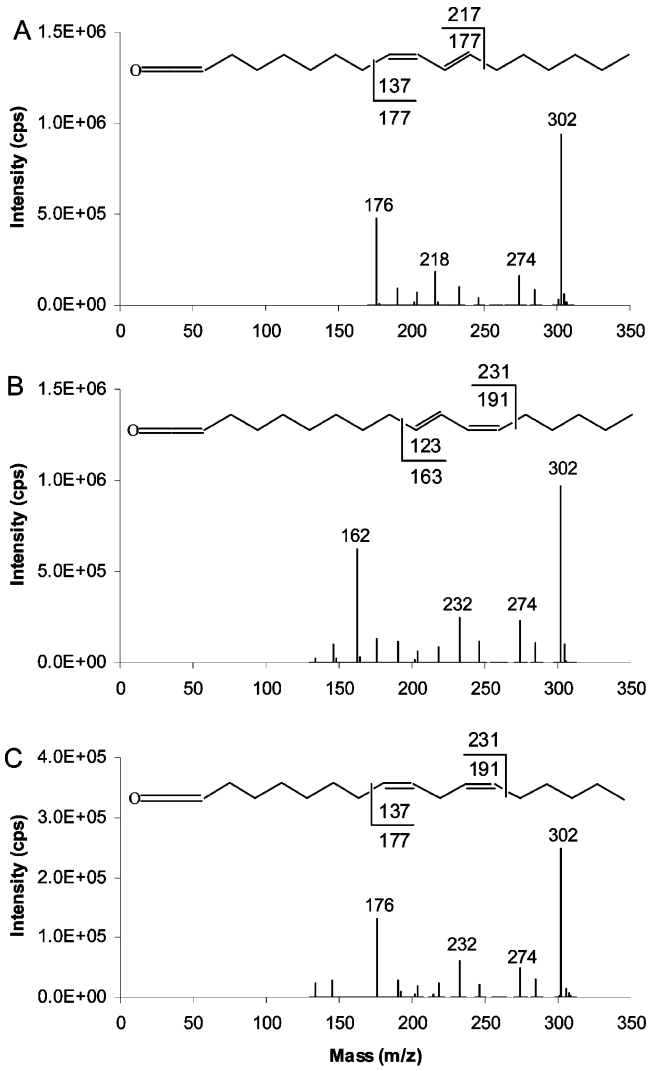

Figure 10. $[M + 40]^+$-based APCACI-MS/MS/MS spectra of (A) (16:0/9,11-18:2/9,11-18:2)-TAG, (B) (16:0/10,12-18:2/10,12-18:2)-TAG, and (C) (16:0/9,12-18:2/9,12-18:2)-TAG. The $[\text{ketene} + 40]^+$ ions at *m/z* 302 derived from $[M + 40]^+$ of diene TAGs (*m/z* 895 → 302 → products) yield two fragments characteristic of the double bond position.

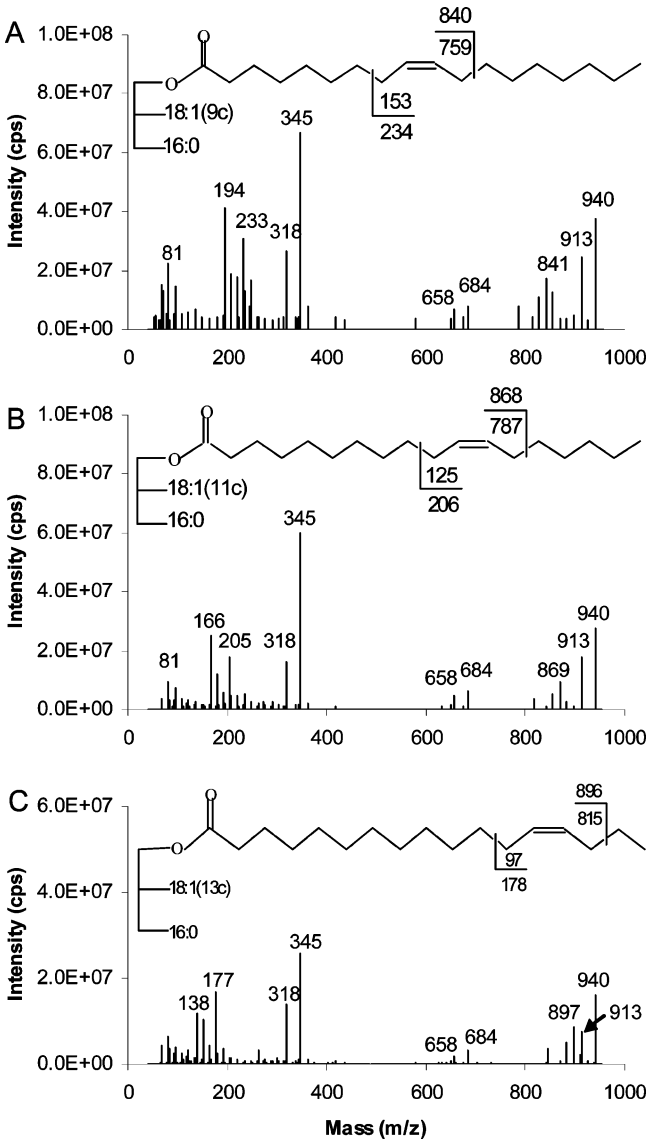

Figure 11. $[M + 81]^+$-based APCACI-MS/MS spectra of (A) (16:0/9-18:1/9-18:1)-TAG (B) (16:0/11-18:1/11-18:1)-TAG, and (C) (16:0/13-18:1/13-18:1)-TAG. Specific cleavages at the allylic carbons shown in the structures at the top of each spectrum give rise to a pair of diagnostic ions. Ions at *m/z* 194 (A), *m/z* 166 (B), and *m/z* 138 (C) correspond to ω diagnostic ions of $[M + 54]^+$, which appears at *m/z* 913 in all spectra.

ions at *m/z* 302 derived from MS/MS of $[M + 40]^+$ of TAGs containing conjugated dienes produces a pair of diagnostic ions resulting from C−C bond cleavage at a position that is vinylic to either site of the conjugated diene unit. A single hydrogen atom is transferred to the charged fragment during α diagnostic ion formation, while a single hydrogen atom is transferred to the neutral fragment during ω diagnostic ion formation. CAD of $[RCH{=}C{=}O + 40]^+$, where R is derived from 9,11-18:2, yields α diagnostic ions at *m/z* 218 and ω diagnostic ions at *m/z* 176, as shown in Figure 10A, whereas that of $[RCH{=}C{=}O + 40]^+$ of 10,-12-18:2 gives ions at *m/z* 232 and 162, respectively (Figure 10B). Figure 10C shows that CAD of the $[RCH{=}C{=}O + 40]^+$ ion, a ketene containing a 9,12-18:2 fatty acyl group, yields an α diagnostic ion at *m/z* 232 and an ω diagnostic ion at *m/z* 176 originating from C−C bond cleavage at a position that is vinylic to each double bond. As with the TAG containing conjugated dienes, the α ions appear 1 unit above the expected mass while ω ions appear at masses 1 unit lower than those expected from homolytic cleavage. In all three spectra, an ion occurring at *m/z* 274 is also apparent. This ion represents a neutral loss of 28 Da from the $[\text{ketene} + 40]^+$ ion, likely to be either CO or ethylene.

$[M + 81]^+$. *APCACI-MS/MS of Monoene-Containing TAGs.* Figure 11 presents results from CAD of $[M + 81]^+$. The spectra are dominated by ions at *m/z* 345 arising from the adducts of ketene and *m/z* 81 ions $[RCH{=}C{=}O + 81]^+$. Each spectrum consists of products at *m/z* 684 and 658 arising by neutral loss of palmitic acid (16:0) and octadecenoic acid (18:1), respectively, from $[M + 81]^+$.

Diagnostic ions corresponding to cleavage adjacent to either allylic site of the double bond were observed. For (16:0/9-18:1/9-18:1)-TAG (Figure 11A), the ion appearing at *m/z* 841 is the α diagnostic ion and that at *m/z* 233 is the ω diagnostic ion. Similarly, parts B and C of Figure 11 show diagnostic ions for

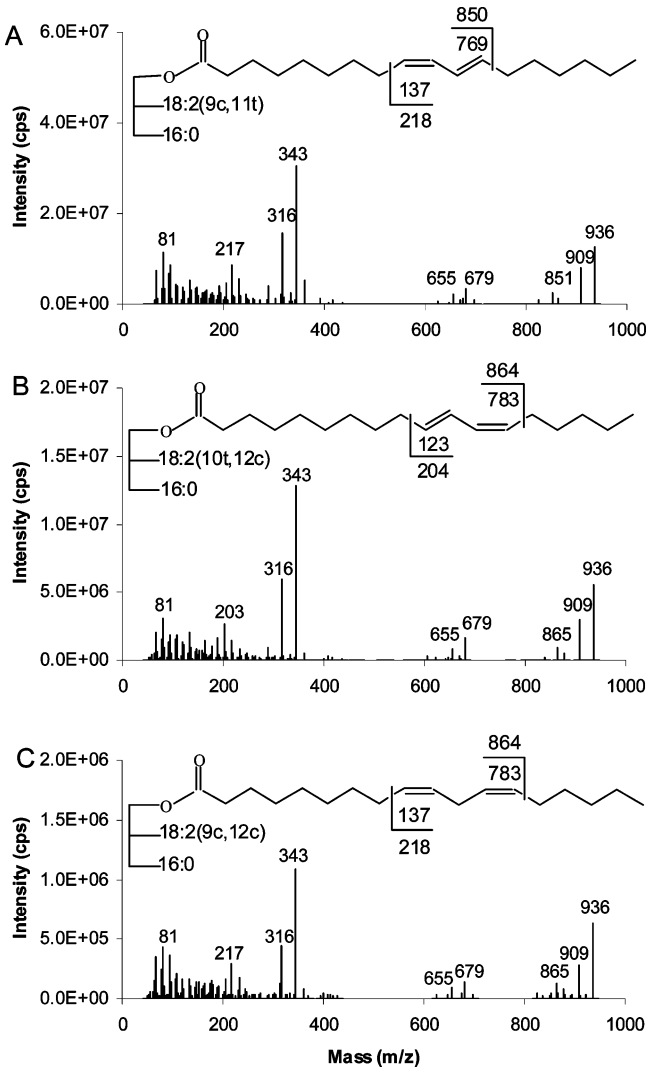

Figure 12. $[M + 81]^+$-based APCACI-MS/MS spectra for *m/z* 936 of (A) (16:0/9,11-18:2/9,11-18:2)-TAG, (B) (16:0/10,12-18:2/10,12-18:2)-TAG, and (C) (16:0/9,12-18:2/9,12-18:2)-TAG. Cleavages directly before the first double bond and immediately after the second, as shown in the structures, give rise to diagnostic ions.

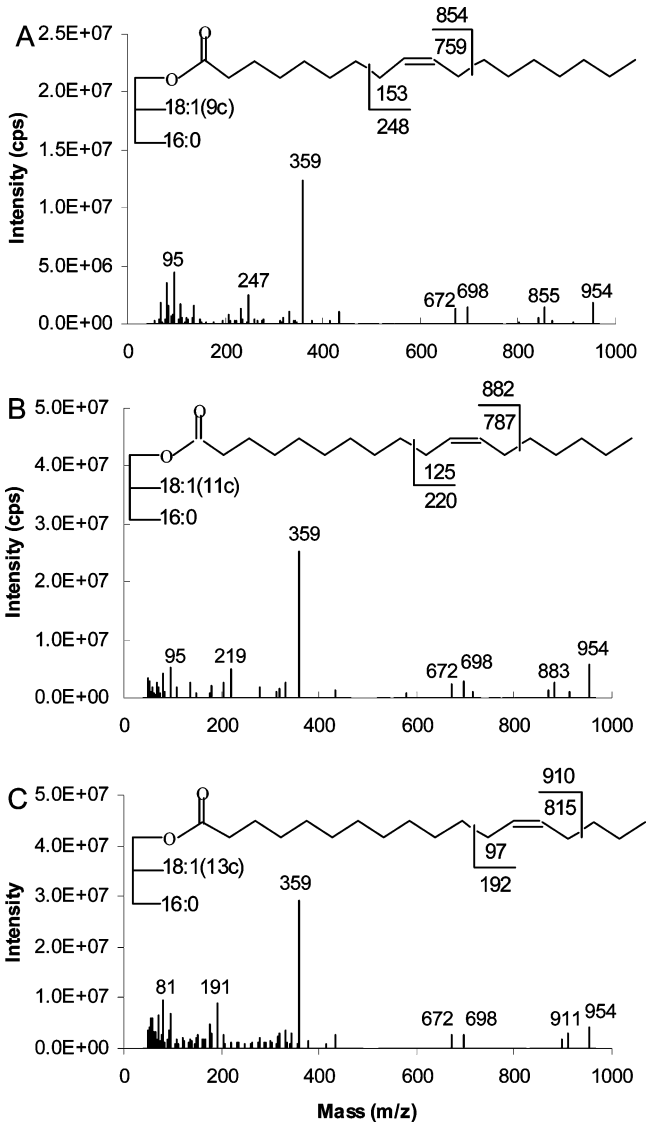

Figure 13. $[M + 95]^+$-based APCACI-MS/MS spectra for *m/z* 954 of (A) (16:0/9-18:1/9-18:1)-TAG, (B) (16:0/11-18:1/11-18:1)-TAG, and (C) (16:0/13-18:1/13-18:1)-TAG. Specific cleavages at the allylic carbons shown in the structures at the top of each spectrum give rise to a pair of diagnostic ions.

the fragmentation of (16:0/11-18:1/11-18:1)-TAG at *m/z* 869 and 205 and for the fragmentation of (16:0/13-18:1/13-18:1)-TAG at *m/z* 897 and 177, respectively. The α ions appear 1 unit above the expected mass, while ω ions appear at masses 1 unit lower than those expected from homolytic cleavage. Interestingly, in these spectra, we also found $[M + 54]^+$ diagnostic ions at *m/z* 913 resulting from CAD of $[M + 81]^+$. The latter ion may dissociate to $[M + 54]^+$, which appears in the spectrum at *m/z* 913, and further dissociate to an ω diagnostic ion. The $[RCH{=}C{=}O + 54]^+$ ions at *m/z* 318 were also detected. The ω ions derived from $[M + 54]^+$ for (16:0/9-18:1/9-18:1)-TAG, (16:0/11-18:1/11-18:1)-TAG, and (16:0/13-18:1/13-18:1)-TAG are at *m/z* 194, 166, and 138, respectively. α ions derived from $[M + 54]^+$ may be present at low levels but are isobaric with satellite ions of α derived from $[M + 81]^+$.

APCACI-MS/MS of Diene-Containing TAGs. Figure 12 shows the APCACI-MS/MS spectra for collisional dissociation of $[M + 81]^+$ of TAGs containing 18:2 fatty acyl groups. The ions observed for all TAGs are $[M + 81]^+$ at *m/z* 936, [ketene + 81]$^+$ ion at *m/z* 343, and $[BB]^+$ at *m/z* 679 and $[AB]^+$ at *m/z* 655 arising, respectively, by loss of 16:0 and 18:2 from the $[M + 81]^+$ ions. The $[M + 54]^+$ ion at *m/z* 909 and $[RCH{=}C{=}O + 54]^+$ at *m/z* 316 were also observed, similar to those observed in Figure 11. In parts A and B of Figure 12, APCACI-MS/MS spectra of TAGs containing 9,11 and 10,12 18:2 isomers are presented, respectively. The α and ω diagnostic ions at masses predicted by cleavage vinylic to the former site of the double bond are observed at *m/z* 851 and 217 for (16:0/9,11-18:2/ 9,11-18:2)-TAG and *m/z* 865 and 203 for (16:0/10,12-18:2/10,12-18:2)-TAG. Figure 12C shows the APCACI-MS/MS spectrum of (16:0/9,12-18:2/9,12-18:2)-TAG. The cleavage vinylic to the former double bond gives rise to the diagnostic ions at *m/z* 217 and 865. As usual, the α ions appear 1 unit above the expected mass, while ω ions appear at masses 1 unit lower than those expected from homolytic cleavage.

$[M + 95]^+$. *APCACI-MS/MS of Monoene-Containing TAGs.* Figure 13 shows the APCACI-MS/MS spectra of (16:0/9-18:1/9-18:1)-TAG, (16:0/11-18:1/11-18:1)-TAG, and (16:0/13-18:1/13-18:

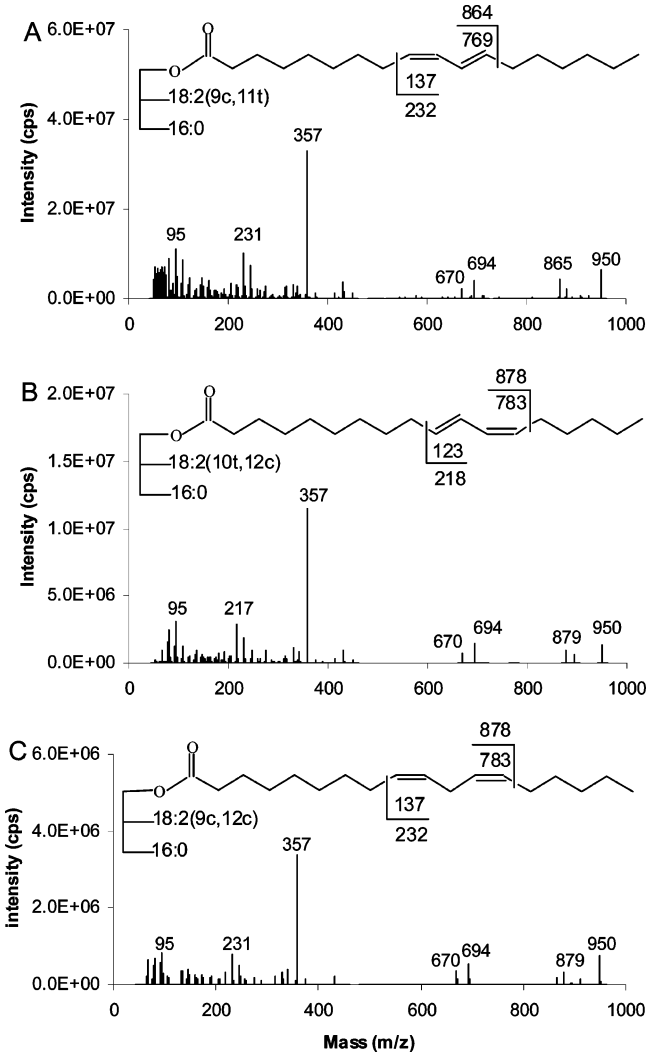

Figure 14. [M + 95]$^+$-based APCACI-MS/MS spectra for *m*/*z* 950 of (A) (16:0/9,11-18:2/9,11-18:2)-TAG, (B) (16:0/10,12-18:2/10,12-18:2)-TAG, and (C) (16:0/9,12-18:2/9,12-18:2)-TAG. Cleavages directly before the first double bond and immediately after the second, as shown in the structures, give rise to diagnostic ions.

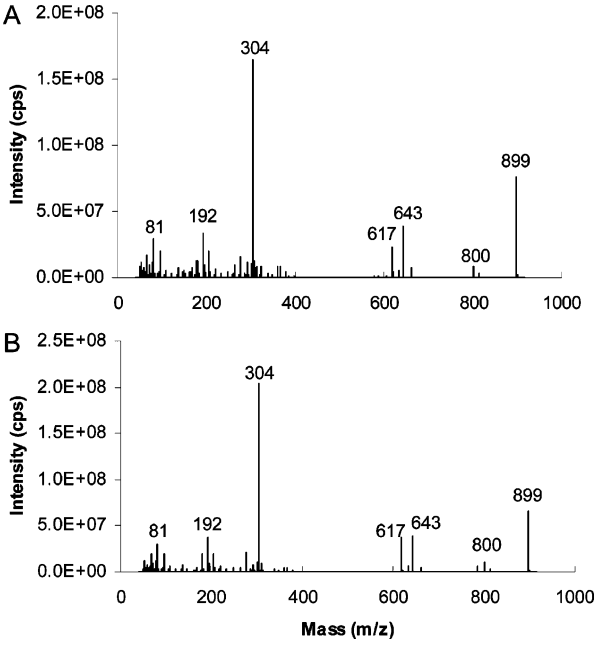

Figure 15. [M + 40]$^+$-based APCACI-MS/MS spectra of *m*/*z* 899 for (A) (16:0/9-18:1/9-18:1)-TAG and (B) (9-18:1/16:0/9-18:1)-TAG. Fragment ions reflecting neutral loss of the *sn*-2 fatty acyl group are less abundant than the corresponding ions reflecting such losses of either the *sn*-1 or *sn*-3 fatty acyl group.

1)-TAG derived from collisional activation of [M + 95]$^+$. The base peaks obtained for all three TAGs are ions at *m*/*z* 357 arising from the adducts of ketene (generated from the fatty acid group) and *m*/*z* 95 ions [RCH=C=O + 95]$^+$. The other ions for all TAGs are *m*/*z* 698 and 672 caused by neutral loss of 16:0 or 18:1, respectively, from the [M + 95]$^+$ ion. Diagnostic ions were formed by allylic cleavage of the double bond, which enables assignment of the double bond position. The α and ω ions are observed at *m*/*z* 855 and 247 for (16:0/9-18:1/9-18:1)-TAG, at *m*/*z* 883 and 219 for (16:0/11-18:1/11-18:1)-TAG, and at *m*/*z* 911 and 191 for (16:0/13-18:1/13-18:1)-TAG. The α ions appear 1 unit above the expected mass, while ω ions appear at masses 1 unit lower than those expected from homolytic cleavage.

APCACI-MS/MS of Diene-Containing TAGs. Collisional activation of [M + 95]$^+$ ions of TAGs containing dienes produces the [RCH=C=O + 40]$^+$ ion at *m*/*z* 357 and [BB]$^+$ at *m*/*z* 694 and [AB]$^+$ at *m*/*z* 670 caused, respectively, by loss of 16:0 and 18:2 from the [M + 95]$^+$ ions, as presented in Figure 14. The α and ω diagnostic ions appear at masses predicted by cleavage vinylic to the double bonds.

As shown in parts A anc B of Figure 14, the α and ω diagnostic ions for (16:0/9,11-18:2/9,11-18:2)-TAG are observed at *m*/*z* 865 and 231, respectively, while the analogous ions for (16:0/10,12-18:2/10,11-18:2)-TAG occur at *m*/*z* 879 and 217, respectively. For (16:0/9,12-18:2/9,12-18:2)-TAG, the α and ω diagnostic ions occur at *m*/*z* 879 and 231, respectively, as indicated in Figure 14C. The α ions appear 1 unit above the expected mass, while the ω ions appear at masses 1 unit lower than those expected from homolytic cleavage.

APCACI-MS^3 performed on ketene adduct peaks for the [M + 81]$^+$ and [M + 95]$^+$ ions yielded low signal-to-noise ratio spectra, even though the [M + 81]$^+$ and [M + 95]$^+$ intensities were similar to those of [M + 40]$^+$ and [M + 54]$^+$ that produced high-quality spectra.

Positions of Acyl Groups on the Glycerol Backbone. The relative intensities of neutral loss of fatty acyl groups or ketenes from TAGs have long been known to be related to their relative positions (*sn*-2 vs *sn*-1,3) in conventional ESI-MS/MS analysis. In APCACI-MS/MS, the neutral loss of a fatty acyl group from [M + 40]$^+$ of a TAG yields [M + 40 − RCO_2]$^+$, while the neutral loss of a fatty acyl group from [M + 54]$^+$ of a TAG yields [M + 54 − RCO_2]$^+$. We tested whether intensity ratios would yield similar regiospecific information for these ions.

The MS/MS spectra of [M + 40]$^+$ of ABB- and BAB-type TAGs containing 16:0 and 9-18:1 fatty acyl groups are given in Figure 15. The ions at *m*/*z* 643 and 617 reflect neutral losses of substituent 16:0 and substituent 9-18:1, respectively. The results indicate that an ABB TAG produces a [BB + 40]$^+$/[AB + 40]$^+$ ratio of 1.68 ± 0.08, whereas a BAB TAG gives 1.06 ± 0.07. Figure 16 shows similar data for the [M + 54]$^+$ adducts. The ions at *m*/*z* 657 and 631, formed by neutral loss of 16:0 or 18:1, respectively, yield [BB + 54]$^+$/[AB + 54]$^+$ ratios of 1.69 ± 0.09

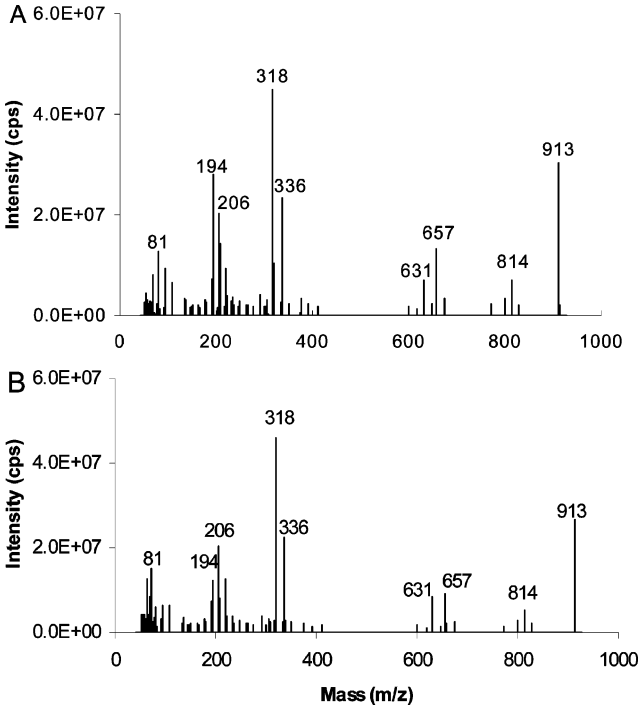

Figure 16. $[M + 54]^+$-based APCACI-MS/MS spectra of *m/z* 913 for (A) (16:0/9-18:1/9-18:1)-TAG and (B) (9-18:1/16:0/9-18:1)-TAG. Fragment ions reflecting neutral loss of the *sn*-2 fatty acyl group are less abundant than the corresponding ions reflecting such losses of either the *sn*-1 or *sn*-3 fatty acyl group.

Table 1. $[BB + 40]^+/[AB + 40]^+$ and $[BB + 54]^+/[AB + 54]^+$ Ratios in BAB- and ABB-Type TAGs, Where A Is 16:0 and B Is a Monoene or Diene Unsaturated Fatty Acyl Substituent, Respectively

	$[BB+40]^+/[AB+40]^+$	$[BB+54]^+/[AB+54]^+$
ABB		
16:0/9-18:1/9-18:1	1.68 ± 0.08	1.69 ± 0.09
16:0/9E,12E-18:2/9E,12E-18:2	1.61 ± 0.10	1.58 ± 0.10
16:0/9,11E-18:2/9,11E-18:2	1.73 ± 0.11	1.78 ± 0.10
Mean±SD	1.67 ± 0.06	1.68 ± 0.10
BAB		
9c-18:1/16:0/9-18:1	1.06 ± 0.07	1.08 ± 0.12
9,12-18:2/16:0/9,12-18:2	1.10 ± 0.09	1.12 ± 0.14
9,11E-18:2/16:0/9,11E-18:2	1.13 ± 0.12	1.02 ± 0.13
Mean±SD	1.10 ± 0.04	1.07 ± 0.05

and 1.08 ± 0.12 for TAGs of the forms ABB and BAB, respectively. Table 1 presents similar data in summary form for six different TAGs, yielding highly reproducible and consistent ratios.

We have published extensively on the reaction and fragmentation of MIE (*m/z* 54) with FAMEs using a gas chromatography introduction into an internal ionization 3D ion trap. This gas-phase implementation of CACI is able to fully determine double bonds in all homoallylic (methylene-interrupted) FAMEs including those at very low concentration. It also determines the double bond position and geometry in conjugated diene FAMEs and in many FAMEs of unusual double bond structure. In FAME CACI spectra, the major adduct ion is $[M + 54]^+$,[40, 49] with smaller amounts of $[M + 40]^+$. $[M + 54]^+$ has proven most useful for locating double bonds. Collisional dissociation of $[M + 54]^+$ yields two diagnostic ions that are indicative of the double bond position for homoallylic FAMEs,[39] and the ion intensities provide information on the double bond geometry in the specific case of conjugated dienes.[42] Mechanistic and structural work indicates that the MIE ion can add to the double bond in a parallel or an antiparallel manner, which determines subsequent fragmentation and H transfer.[41] In all cases studied to date, H transfer is symmetric with respect to the ion or neutral loss: in the case of monoenes and dienes, the H transfer is to the ion, whereas H transfer is to the neutral group with polyenes for both the α and ω ions. Here we observe that H transfer is always *to* the α ion and *away* from the ω ion. This result has no analytical consequences but may reflect a mechanism or structure different from that found for FAME $[M + 54]^+$.

Cleavage sites of TAG adducts follow a clear pattern, similar to that observed for FAME $[M + 54]^+$ ions. Cleavage is allylic to the site of the erstwhile double bond of monoene-containing TAGs for all α ions and for ω ions from $[M + 40]^+$, $[M + 81]^+$, and $[M + 95]^+$. Cleavage is both allylic and vinylic for ω ions from $[M + 54]^+$, and $[M + 81]^+$ dissociates to yield ω ions at the same masses as $[M + 54]^+$. For diene-containing TAGs, vinylic cleavage is observed for both α and ω ions.

The $[M + 40]^+$ ion appears to be the best choice for analysis. The intensity of this adduct is slightly greater than that of $[M + 54]^+$ in the MS mode. More importantly, the MS^3 intensity for the ketene fragmentation is most intense of all the adducts, about double that of the $[M + 54]$ ketene ion. Finally, the $[M + 40]^+$ adduct yields two strong diagnostic ions in MS/MS, both due to allylic cleavage, whereas $[M + 54]^+$ yields an extra ω ion due to vinylic cleavage which slightly complicates the spectrum.

SUMMARY

APCACI using acetonitrile as an APCI reagent has been shown to be an effective method to obtain detailed structural information of TAGs, including the location of double bonds along acyl groups and the position of acyl groups on the glycerol backbone. In addition to ions at *m/z* 40 and 54, ions at *m/z* 81 and 95 were observed. These ions appear to form a charged covalent adduct across carbon−carbon double bonds in TAGs containing unsaturated fatty acyl groups, analogous to those observed for FAMEs. Collisionally activated dissociation of the $[M + 40]^+$, $[M + 54]^+$, $[M + 81]^+$, and $[M + 95]^+$ ions yields two or three diagnostic ions similar to those observed previously in FAME analysis.

With few exceptions, fragmentation behavior is similar for all four ions. For monoenes, the α ions containing the glycerol moiety yield strong fragments at the site allylic to the erstwhile double bond. For the ω ions containing the terminal methyl group of the fatty acyl chain, fragmentation is primarily allylic to the former site of the double bond for $[M + 40]^+$ and $[M + 95]^+$ and both vinylic and allylic for $[M + 54]^+$ and $[M + 81]^+$. For dienes, cleavage is vinylic to the site of the former double bond for all adducts and for both α and ω ions. In all cases of monoenes and dienes, a H is transferred from the neutral group to the α ions, but is transferred away from the ω ions.

The fragmentations of ketene adduct $[RCH{=}C{=}O + 54]^+$ or $[RCH{=}C{=}O + 40]^+$ in MS^3 yields two strong diagnostic ions that locate the position of double bonds along fatty acyl chains. Finally, the ratios of $[BB + 40]^+$ to $[AB + 40]^+$ and $[BB + 54]^+$ to $[AB +$

54]$^+$ enable determination of the fatty acyl group regiospecificity on the glycerol backbone. It is left to future work to establish whether this approach can determine the structures of other glycerolipids.

The extended plasma discharge observed with the present APCI ion source appears to be essential for production of sufficient reagent ions for reaction. While it is possible to run the source under these conditions for an extended period, a redesign of the source is probably required to contain the reactive plasma within a volume distant from the metal heater and other parts vulnerable to degradation with extended plasma exposure.

ACKNOWLEDGMENT

This work was supported by NIH Grant GM071534.

Received for review November 2, 2006. Accepted December 21, 2006.

AC062055A